analytical chemistry

Article

pubs.acs.org/ac

Photoemission Electron Microscopy and Scanning Electron Microscopy of *Magnetospirillum magnetotacticum*'s Magnetosome Chains

Christoph Keutner,*[,†,‡] Alex von Bohlen,[¶] Ulf Berges,[†,‡] Philipp Espeter,[†,‡] Claus M. Schneider,[§] and Carsten Westphal[†,‡]

[†]Experimentelle Physik 1, Technische Universität Dortmund, Otto-Hahn-Strasse 4, D-44221 Dortmund, Germany
[‡]DELTA, Technische Universität Dortmund, Maria-Goeppert-Mayer-Strasse 2, D-44221 Dortmund, Germany
[¶]Leibniz-Institut für Analytische Wissenschaften—ISAS—e.V., Bunsen-Kirchhoff-Strasse 11, D-44139 Dortmund, Germany
[§]Peter Grünberg Institut, PGI-6, Forschungszentrum Jülich GmbH, D-52425 Jülich, Germany

ABSTRACT: Magnetotactic bacteria are of great interdisciplinary interest, since a vast field of applications from magnetic recording media to medical nanorobots is conceivable. A key feature for a further understanding is the detailed knowledge about the magnetosome chain within the bacteria. We report on two preparation procedures suitable for UHV experiments in reflective geometry. Further, we present the results of scanning electron microscopy, as well as the first photoemission electron microscopy experiments, both accessing the magnetosomes within intact magnetotactic bacteria and compare these to scanning electron microscopy data from the literature. From the images, we can clearly identify individual magnetosomes within their chains.

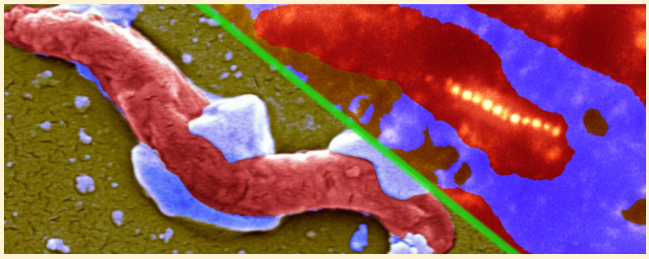

The bacteria *Magnetospirillum magnetotacticum* (MS-1)[1] is a Gram-negative, amphitrichous representative of the group of magnetotactic bacteria (MTB). By a biochemically controlled process called biomineralization,[2,3] the MTB form a chain of membrane-bounded, intracellular magnetic nanoparticles consisting of ferrimagnetic magnetite (Fe_3O_4)[4] or greigite (Fe_3S_4).[5] The arrangement and formation of these magnetosomes is primarily biologically regulated,[6,7] although environmental factors are not negligible.[8−11] These chains enable the MTB to find efficiently the microaerobic region, which provides optimal chemical conditions for their metabolism,[12] by aligning the MTB along the geomagnetic field[1,13] and thus allowing only movements parallel to it.[14] Single magnetosomes of MS-1 consist of magnetite crystals of 35−120 nm average in size.[2,15]

In technological, medical, and environmental science magnetosomes are considered as a perspective material because of their narrow size and chemical purity. Possible new applications include magnetic recording media, magnetic resonance imaging,[16] and medical nanorobots.[17,18] Because of these manifold application possibilities, MTB of all species and their magnetosomes are of particular, interdisciplinary interest. Therefore, various different investigation methods were applied to these bacteria. These include, among other techniques ferromagnetic resonance,[19,20] transmission electron microscopy,[6,10] and electron holography.[21,22] However, other experimental methods such as magnetic force microscopy,[17] differential phase contrast microscopy,[23] and SQUID magnetometry[24] allow only access to magnetosomes being extracted from the bacteria. Further, it is important to distinguish results obtained by methods using entire bacteria or obtained from extracted magnetosome chains,[25,26] since their properties differ significantly.[27]

Among all techniques applied to MTB in the past, two techniques providing spatial, chemical, and even magnetic information are missing, to the best of our knowledge. These are photoemission electron microscopy (PEEM) and scanning electron microscopy in combination with energy dispersive X-ray spectrometry (SEM-EDX). Although SEM images of intact MTB exist, the only known images recorded by secondary electron emission showed hints of magnetosome chains for wildtype magnetic cocci.[28] There, the magnetosome chains were identified as bulges of the cell envelope. Recently, backscattered electrons from SEM experiments showed the magnetosome chain within the MTB.[29] From those SEM images it was not possible to identify individual magnetosomes or to resolve the chain sharply. Hence, the MTB had to be sectionized or cryofractured to achieve a clear image of the magnetosomes. Summarizing, neither the magnetosome chain nor single magnetosomes were sharply imaged within an intact MTB up to now.

Received: June 4, 2014
Accepted: September 2, 2014

   dx.doi.org/10.1021/ac502050j | *Anal. Chem.* XXXX, XXX, XXX−XXX

For further investigations in this field an analytical tool is required for studying MTB on more complex substrates than the normally used grids. PEEM could be a suitable method for this task. With a resolution of a micrometer and below, it can image the magnetization of each magnetosome directly, rather than displaying field lines as holographic techniques do. Combined with PEEM's time resolution dynamical studies on MTB's response to external stimulations might be possible, in the future. Very recent PEEM results show a lateral resolution of 10 nm for Co/Pd multilayer samples.[30] Therefore, a suitable preparation method for intact bacteria on a solid substrate has to be developed. Further, it has to be clarified if the magnetosome chains can be investigated by this technique.

In PEEM, the sample's emitted photoelectrons are mapped in order to image the sample surface.[31] For rather low photon energies only electrons of valence states are excited. This "threshold-emission mode" yields the highest image resolution. Besides topographic features, differences in the work function dominate this mode. In the high-energy mode, core level electrons are excited. Therefore, it is possible to measure spatially resolved X-ray absorption spectra (XAS).[32,31] In these spectra, the photoelectron yield of a specific region of interest (ROI) is recorded as a function of the photon excitation energy.[33] Thus, PEEM combines basic microscopic techniques with spectroscopic features providing spatially and spectrally resolved information on the sample.

EXPERIMENTAL SECTION

The first PEEM measurements of MTB were preformed using a STAIB-PEEM-350 in threshold-emission mode ($h\nu$ = 4.9 eV). Thus, the main contrast is obtained from differences in the work function, and the surface's topographical profile. Further measurements were carried out at the SGM-beamline 4-ID-C at the APS, providing circularly polarized synchrotron radiation. Therefore, distinct chemical signals are accessible by using an Omicron-Focus PEEM. The system for the SEM-EDX measurements combines an SEM Quanta 200 FEG from FEI, and an EDX spectrometer Quantax 400 SDD X-Flash 4010, with an energy resolution of 123 eV at Mn−K_α supplied by Bruker.

RESULTS AND DISCUSSION

Sample Preparation. Cultures of the MS-1 were purchased from DSMZ[34] as an actively growing culture in liquid medium. A first enrichment of the bacteria was achieved from their natural tendency of moving toward the oxic−anoxic transition zone.[9] In order to start this migration within the medium, the airtight sealing was opened. Next, the culture tube was slightly dandled until the clear, transparent medium started changing its color into a faint pink-purple. Then, the tube was stored at a dark place for 46 h at room temperature. As a result, the bacteria accumulated a few millimeters beneath the medium surface in a milky layer of approximately 1 mm thickness. In the subsequent preparation steps two different methods were tried.

First, in order to achieve a very high bacteria density, 1 mL of the bacteria rich layer was extracted and centrifuged at 4 °C with a relative centrifugal force (RCF) of 10 000 × g for 15 min. In this step the extract was separated into a fluid phase floating above a jelly like phase. The jelly phase was washed in 1 mL of phosphate buffered saline (PBS, pH = 7.4) for 5 min at RFC = 10 000 × g and 4 °C. The washed jelly phase was then resuspended by adding 0.5 mL of PBS. This bacteria−PBS mixture was diluted and applied onto the sample carrier, and air-dried. In order to achieve a high bacteria density with a low content of media residuals, test preparation sequences on microscope slides as well as on Si(100)-wafers were preformed. As a result, an ideal dilution of the bacteria-PBS mixture with distilled water of a 1:10 ratio was obtained. However, we still found several surface regions which were mainly covered by salt crystals from the dried PBS, partially burying the bacteria as shown in Figure 1. Since these salt crystals could cause sample

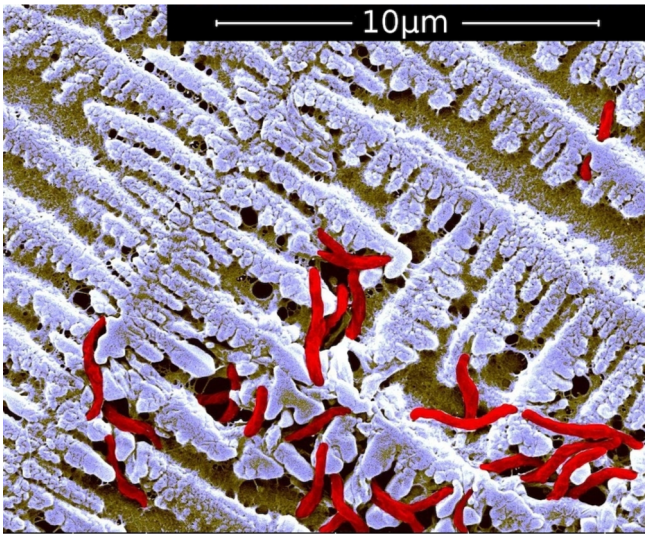

Figure 1. False color SEM image of a gold coated sample surface, prepared with the bacteria−PBS mixture. The bacteria (red) are entangled in a structure of PBS crystals (violet).

charging, resulting in image distortions during PEEM measurements, the dried sample surface was rinsed with 0.4 mL of distilled water, leaving only a few impurities at the surface, as displayed in Figure 2.

The second preparation procedure omitted applying centrifugation and washing sequences, at the expense of the

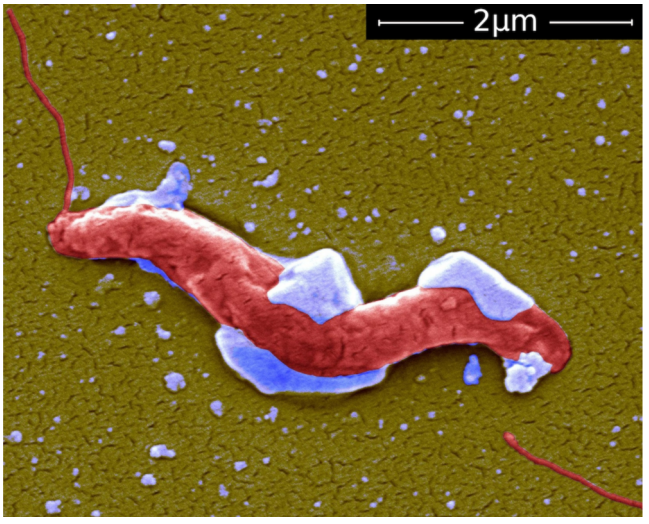

Figure 2. MS-1 (red) after rinsing the dried sample, reducing the PBS crystals (violet). The two polar flagella are clearly visible, with one separated from the body. The sample was coated by a few monolayers of gold.

dx.doi.org/10.1021/ac502050j | Anal. Chem. XXXX, XXX, XXX−XXX

bacteria density. The bacteria–medium mixture was directly extracted from the milky layer and diluted with distilled water, applied to the sample carrier, and air-dried. Although, the dilution step reduces the bacteria density it was necessary to lessen the content of media residuals, as mentioned above.

PEEM Measurements. The first set of PEEM measurements was carried out in order to find out in how far bacteria in general and MS-1 in particular are accessible by means of PEEM. Especially, the critical question of charging effects in the absence of any gold coating needed to be clarified. Fortunately, these effects can be neglected as demonstrated in Figure 3, showing a clear image of regions with multiple bacteria which were surrounded by flat, residual free areas.

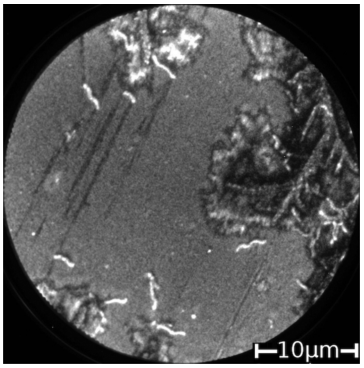

Figure 3. Threshold PEEM-image of MS-1 (bright) on a Si surface (light gray). The salt residuals are visible as inhomogeneous, high contrast regions, containing additional bacteria.

For the second set of measurements being carried out at the Advanced Photon Source (APS), Argonne, all samples were prepared according to the second preparation procedure. Although the bacteria density is lower, there are still bunches of bacteria on a nearly clean surface with only few media residuals, as Figure 4 shows.

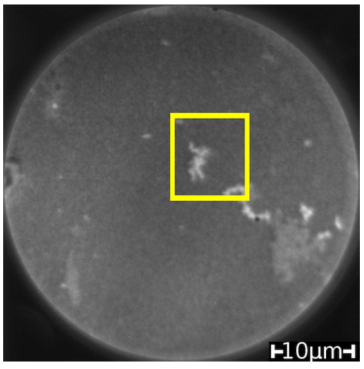

Figure 4. PEEM-image of a sample prepared at the APS. Two bunches of bacteria are clearly visible in the center of the image. The yellow box indicates the region shown in Figure 5.

Figure 5 is the superposition of an image sequence, recoded for excitation energies from $h\nu$ = 703 to 707 eV in increments of 0.2 eV. XAS Fe L_3-spectra, displayed in the upper panel of Figure 6, were extracted from the indicated ROIs, representing the bacteria bunch and the uncovered sample surface, respectively. To remove the background, the intensity difference between ROI A and ROI B was calculated for each excitation energy. The difference between these two spectra is

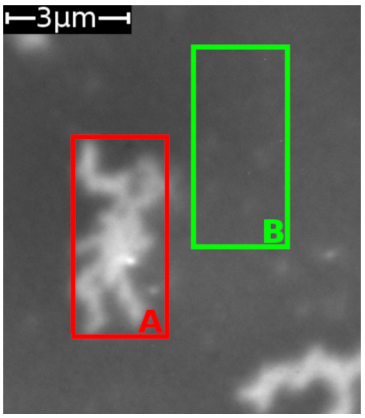

Figure 5. Indicated region in Figure 4 with enhanced magnification. Regions of interest (ROI) A and B are of the same size and indicated by a red and a green box, respectively.

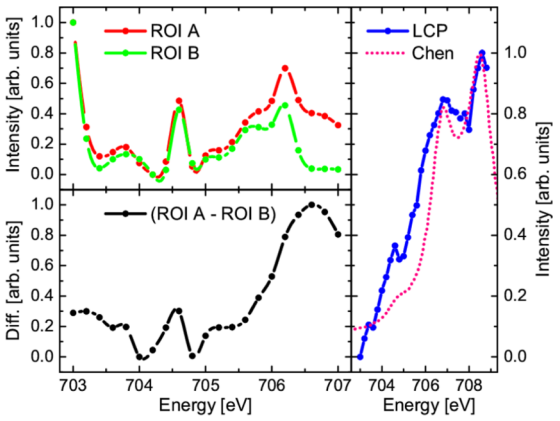

Figure 6. Upper panel: XAS spectra extracted from the ROIs shown in Figure 5. Lower panel: Difference signal of the two spectra. Right panel: Spectrum extracted from an image sequence recorded with left circularly polarized light (LCP). The spectrum calculated by Chen et al.[35] is added for ease of comparison.

shown in the lower panel of Figure 6, adjusted to the range [0,1]. Although the iron containing magnetosomes are representing just a very small fraction of the bacteria, a clear signal of magnetite is visible. A similar result is shown in the right panel of Figure 6, where left circularly polarized light in the energy range of 703.0 to 708.8 eV was used for excitation. Now, structures at an energy of 704.6, 706.8, and 708.6 eV are visible, in excellent agreement with recent calculations.[35] These features of the XAS are induced by the magnetite's magnetic circular dichroism and therefore demonstrating the accessibility of the magnetosomes by means of PEEM.

SEM-EDX Measurements. Complementary to the PEEM measurements the samples were examined by SEM-EDX. Because of the electrons' low escape length, any additional gold coating would reduce the probing depth. Since, the magnetic particles are located in the bacterium's center, this would prevent their detection, as seen in Figures 1 and 2. Hence, any gold coating should be omitted. Fortunately, no charging effects were observed as verified by the PEEM results reported above. Also, SEM-images of noncoated samples showed no charging, as shown in Figure 7. The absence of a gold coating allows an imaging of single magnetosome chains within the bacteria, clearly displaying individual magnetosomes. However, roughly half of all depicted bacteria show no clear signal of a

dx.doi.org/10.1021/ac502050j | Anal. Chem. XXXX, XXX, XXX–XXX

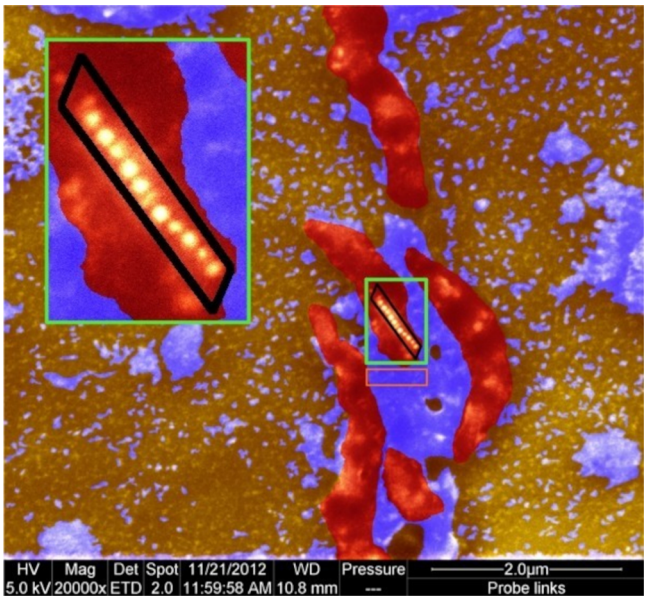

Figure 7. False color SEM image of four MS-1 (red) on Si (gold), surrounded by remaining solution components (blue). A magnetosome chain is clearly visible (green box, inset). The regions for the SEM-EDX measurements are marked by a black and an orange box.

magnetosome chain at all. This is probably caused by the position of the magnetosome chain near the cell envelope,[36] in these cases at the bottom side of the bacteria.

For the SEM-EDX measurements, two ROIs were chosen representing the magnetosome chain and a reference region as indicated by the black and orange boxes in Figure 7, respectively. The corresponding spectra are displayed in the upper panel of Figure 8, with a close-up view of the Fe $L_{\alpha,\beta 1}$-signal. The lower panel represents the difference obtained from the magnetosome chain and reference region signals. The most significant differences are displayed for the organic components

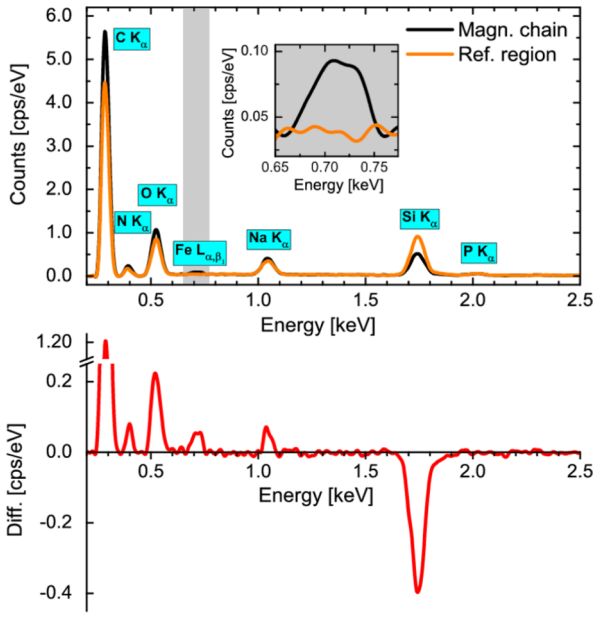

Figure 8. Upper panel: SEM-EDX spectra for the magnetosome chain and the reference region. The indicated part of the spectra is shown in the close-up inset. Lower panel: Difference of the two spectra.

C and O, with a high concentration of those within the bacterium, and the reduced Si-signal compared to the reference region. Although the iron signal is rather small compared to the other signals, the mass percentage increases drastically for the magnetosome chain as shown in Table 1, since the reference region contains no iron. The absence of a S K_α-signal at 2.3 keV confirms that the magnetosomes consist of magnetite and not of greigite.

Table 1. Mass Percentage of Different Elements as Determined by SEM-EDX Spectroscopy[a]

mass-%	magn. chain	ref. region
C	71.0	70.8
N	dl	0.2
O	16.7	17.5
Na	1.9	0.9
Si	8.8	10.6
P	0.15	dl
Fe	1.5	dl

[a]dl = values below the detection limit.

The signals of nitrogen displayed in the difference spectra cannot be quantified easily. The first problem is related to the subtraction of the spectral background. The second is related to the lack of standard reference materials for the spectral range in question. For these reasons, we prefer to use the implemented set of standard parameters of the evaluation software. Uncertainties can be estimated and are of about one to two percent relative. The detection limits are strongly influenced by the local distribution of the elements, by the matrix material, and by the analytical parameters.

The reduced silicon signal can be explained by a lower sampling depth caused by the magnetite. A line-scan along the magnetosome chain shows a nearly inverse variation of the Si and Fe signals, as displayed in Figure 9. Here, no sharp contrast is displayed, since the spatial resolution is limited by the excited volume, and probing depth of the emitted characteristic radiation.

CONCLUSIONS

In conclusion, we present two methods of preparing MS-1. One method is rather time-consuming, yielding a high bacteria density. The alternative route is simpler and faster, at the expense of bacteria density. Both preparation methods showed intact bacteria with their in vivo structure, as demonstrated by

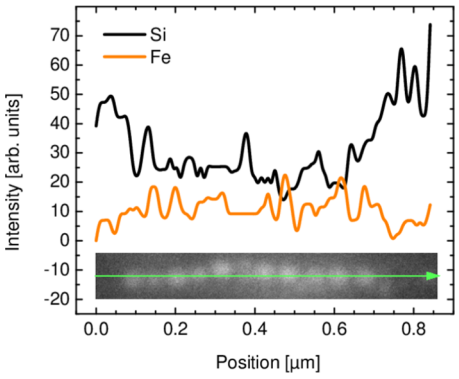

Figure 9. Line scan along the magnetosome chain (green line, inset) for Si and Fe.

dx.doi.org/10.1021/ac502050j | Anal. Chem. XXXX, XXX, XXX−XXX

SEM-pictures. We presented the first PEEM images of MTB. Further, XAS spectra are in excellent agreement with calculations,[35] demonstrating that the magnetosome chains can be investigated by this technique. Thus, PEEM might be a new method for accessing the magnetosome chain within the MTB. Since each point of the entire image is acquired simultaneously and without scanning, this could become beneficial for studies of dynamic processes. These could be, for instance, the magnetosome chain's response to changing magnetic fields, since a physical realignment of the MTB is prevented by their fixed position on the surface. By application of identical preparation methods, we also report on the first SEM images in which the magnetosome chains of intact bacteria are directly visible, and we further show that single magnetosomes are distinguishable within these chains. Since the magnetosome chain of MS-1 lies near the cell envelope[36] and roughly half of the MTB show no magnetosome chain, the sampling depths can be estimated to approximately half of the bacterium's diameter.

AUTHOR INFORMATION

Corresponding Author

*E-mail: christoph.keutner@tu-dortmund.de.

Notes

The authors declare no competing financial interest.

ACKNOWLEDGMENTS

This work was funded by the Land Nordrhein-Westfalen and the NRW Research School of Synchrotron Radiation in Nano- and Biosciences. Use of the Advanced Photon Source was supported by the U.S. Department of Energy, Office of Science, Office of Basic Energy Sciences, under Contract No. W-31-109-Eng-38. We thank S. Brakmann for advice on bacteria handling, and D. J. Keavney for assistance using beamline 4-ID-C. The authors thank the DELTA and APS staff for the support during beamtimes.

REFERENCES

(1) Blakemore, R. *Science* **1975**, *190*, 377.
(2) Schüler, D. *BIOspektrum* **2000**, *6*, 445.
(3) Bazylinski, D. A.; Frankel, R. B. *Rev. Mineral. Geochem.* **2003**, *54*, 217.
(4) Frankel, R. B.; Blakemore, R. P.; Wolfe, R. S. *Science* **1979**, *203*, 1355.
(5) Heywood, B. R.; Bazylinski, D. A.; Garratt-Reed, A.; Mann, S.; Frankel, R. B. *Naturwissenschaften* **1990**, *77*, 536.
(6) Komeili, A.; Vali, H.; Beveridge, T. J.; Newman, D. K. *Proc. Natl. Acad. Sci. U.S.A.* **2004**, *101*, 3839.
(7) Scheffel, A.; Gruska, M.; Faivre, D.; Linaroudis, A.; Plitzko, J. M.; Schüler, D. *Nature* **2006**, *440*, 110.
(8) Bazylinski, D. A. *Chem. Geol.* **1996**, *132*, 191.
(9) Bazylinski, D. A.; Frankel, R. B. *Nat. Rev. Microbiol.* **2004**, *2*, 217.
(10) Bazylinski, D. A.; Dean, A. J.; Williams, T. J.; Long, L. K.; Middleton, S. L.; Dubbels, B. L. *Arch. Microbiol.* **2004**, *182*, 373.
(11) Schüler, D.; Baeuerlein, E. *J. Bacteriol.* **1998**, *180*, 159.
(12) B. Frankel, R.; A. Bazylinski, D.; S. Johnson, M.; L. Taylor, B. *Biophys. J.* **1997**, *73*, 994.
(13) Bazylinski, D. A.; Moskowitz, B. M. *Rev. Mineral. Geochem.* **1997**, *35*, 181.
(14) Frankel, R. B. *Annu. Rev. Biophys. Bioeng.* **1984**, *13*, 85.
(15) Frankel, R. B.; Bazylinski, D. A.; Schüler, D. *Supramol. Sci.* **1998**, *5*, 383.
(16) Lee, Y.; Lee, J.; Bae, C.; Park, J.-G.; Noh, H.-J.; Park, J.-H.; Hyeon, T. *Adv. Funct. Mater.* **2005**, *15*, 503.
(17) Albrecht, M.; Janke, V.; Sievers, S.; Siegner, U.; Schüler, D.; Heyen, U. *J. Magn. Magn. Mater.* **2005**, *290*, 269.
(18) Martel, S.; Mohammadi, M.; Felfoul, O.; Lu, Z.; Pouponneau, P. *Int. J. Rob. Res.* **2009**, *28*, 571.
(19) Charilaou, M.; Winklhofer, M.; Gehring, A. U. *J. Appl. Phys.* **2011**, *109*, No. 093903.
(20) Fischer, H.; Mastrogiacomo, G.; Löffler, J. F.; Warthmann, R. J.; Weidler, P. G.; Gehring, A. U. *Earth Planet. Sci. Lett.* **2008**, *270*, 200.
(21) McCartney, M. R.; Lins, U.; Farina, M.; Buseck, P. R.; Frankel, R. B. *Eur. J. Mineral.* **2001**, *13*, 685.
(22) Simpson, E. T.; Kasama, T.; Pósfai, M.; Buseck, P. R.; Harrison, R. J.; Dunin-Borkowski, R. E. *J. Phys.: Conf. Ser.* **2005**, *17*, 108.
(23) Daykin, A. C.; Petford-Long, A. K. *Ultramicroscopy* **1995**, *58*, 365.
(24) Moskowitz, B. M.; Frankel, R. B.; Bazylinski, D. A. *Earth Planet. Sci. Lett.* **1993**, *120*, 283.
(25) Coker, V. S.; Telling, N. D.; van der Laan, G.; Pattrick, R. A. D.; Pearce, C. I.; Arenholz, E.; Tuna, F.; Winpenny, R. E. P.; Lloyd, J. R. *ACS Nano* **2009**, *3*, 1922.
(26) Staniland, S.; Williams, W.; Telling, N.; van der Laan, G.; Harrison, A.; Ward, B. *Nat. Nanotechnol.* **2008**, *3*, 158.
(27) Alphandéry, E.; Ngo, A. T.; Lefèvre, C.; Lisiecki, I.; Wu, L. F.; Pileni, M. P. *J. Phys. Chem. C* **2008**, *112*, 12304.
(28) Hanzlik, M.; Winklhofer, M.; Petersen, N. *Earth Planet. Sci. Lett.* **1996**, *145*, 125.
(29) Jogler, C.; Wanner, G.; Kolinko, S.; Niebler, M.; Amann, R.; Petersen, N.; Kube, M.; Reinhardt, R.; Schüler, D. *Proc. Natl. Acad. Sci. U.S.A.* **2011**, *108*, 1134.
(30) Ishiwata, H.; Acremann, Y.; Scholl, A.; Rotenberg, E.; Hellwig, O.; Dobisz, E.; Doran, A.; Tkachenko, B. A.; Fokin, A. A.; Schreiner, P. R.; Dahl, J. E. P.; Carlson, R. M. K.; Melosh, N.; Shen, Z.-X.; Ohldag, H. *Appl. Phys. Lett.* **2012**, *101*, No. 163101.
(31) Stöhr, J.; Anders, S. *IBM J. Res. Dev.* **2000**, *44*, 535.
(32) Stöhr, J.; A. Padmore, H.; Anders, S.; Stammler, T.; R. Scheinfein, M. *Surf. Rev. Lett.* **1998**, *5*, 1297.
(33) M. Schneider, C.; Schönhense, G. *Rep. Prog. Phys.* **2002**, *65*, R1785.
(34) Leibniz Institute DSMZ GmbH, 2013. http://www.dsmz.de/.
(35) Chen, J.; Huang, D. J.; Tanaka, A.; Chang, C. F.; Chung, S. C.; Wu, W. B.; Chen, C. T. *Phys. Rev. B* **2004**, *69*, No. 085107.
(36) Martins, J. L.; Keim, C. N.; Farina, M.; Kachar, B.; Lins, U. *Curr. Microbiol.* **2007**, *54*, 1.